

Multi-stage structural damage diagnosis method based on “energy-damage” theory

Ting-Hua Yi^{1,2}, Hong-Nan Li^{*1,2} and Hong-Min Sun³

¹*School of Civil Engineering, Faculty of Infrastructure Engineering, Dalian University of Technology, Dalian 116023, China*

²*State Key Laboratory of Coastal and Offshore Engineering, Dalian University of Technology, Dalian 116023, China*

³*School of Civil Engineering, Shenyang Jianzhu University, Shenyang 110168, China*

(Received July 12, 2012, Revised October 31, 2012, Accepted November 7, 2012)

Abstract. Locating and assessing the severity of damage in large or complex structures is one of the most challenging problems in the field of civil engineering. Considering that the wavelet packet transform (WPT) has the ability to clearly reflect the damage characteristics of structural response signals and the artificial neural network (ANN) is capable of learning in an unsupervised manner and of forming new classes when the structural exhibits change, this paper investigates a multi-stage structural damage diagnosis method by using the WPT and ANN based on “energy-damage” theory, in which, the wavelet packet component energies are first extracted to be damage sensitive feature and then adopted as input into an improved back propagation (BP) neural network model for damage diagnosis in a step by step mode. To validate the efficacy of the presented approach of the damage diagnosis, the benchmark structure of the American Society of Civil Engineers (ASCE) is employed in the case study. The results of damage diagnosis indicate that the method herein is computationally efficient and is able to detect the existence of different damage patterns in the simulated experiment where minor, moderate and severe damages corresponds to involving in the loss of stiffness on braces or the removal bracing in various combinations.

Keywords: damage diagnosis; energy-damage theory; wavelet packet analysis; BP neural network; benchmark structure

1. Introduction

The structural integrity of critical civil infrastructures is of continuing concern to the international engineering community from both economic and life-safety viewpoints (Wenzl 2009, Boller 2009, Yi *et al.* 2012). Structural degradation, whether caused by material aging due to the environment and service loads (fatigue, corrosion, etc.) or by unpredictable external events (earthquakes, impact, etc.), is an inevitable fact of life. Therefore, it's benefit to be gained in the ability to detect, locate, and quantify the damage throughout the civil community. Conventional damage detection methods are visual or localized experimental methods such as ultrasonic,

*Corresponding author, Professor, E-mail: hnli@dlut.edu.cn

magnetic field, radiograph, eddy-current, and thermal field methods (Zhang *et al.* 1999). However, all of these methods require that the vicinity of the damage be known a priori and that the portion of the structure being inspected be readily accessible. Thus, global methodologies, in which the entire structure is excited and the response is measured at certain places, are better suited to the task of locating damage. The basic premise of vibration-based global damage detection methods is that changes in the physical properties (mass, damping and stiffness), such as reductions in stiffness resulting from the onset of cracks or loosening of a connection, will cause changes in the measured dynamic properties of the structure (natural frequencies, mode shapes and amplifications) (Li and Yang 2007).

Global damage detection methods based upon measured vibration characteristics of structures have gotten considerable attention in the last decade. A comprehensive literature review on methods of damage detection and health monitoring using vibration signals for structural and mechanical systems was provided by Doebling *et al.* (1996). Sohn *et al.* (2001) proposed a damage detection approach based on the “statistical pattern recognition” paradigm using time series analysis of vibration signals. This damage detection approach has shown great promise in the hull of a high-speed patrol boat as well as in several relatively simple laboratory test specimens. Sun and Chang (2002) gave a wavelet packet transform (WPT) based method for the damage assessment. Dynamic signals measured from a structure were first decomposed into wavelet packet components in the time domain. Component energies were then calculated and used as inputs into the artificial neural network (ANN) models for the damage assessment. Nair *et al.* (2006) presented a time series algorithm for the damage identification and localization. In contrast to prior pattern classification and statistical signal processing algorithms that have been able to identify primarily severe damage and have not been able to localize the damage effectively, the proposed algorithm is able to identify and localize minor to severe damage. Carden and Brownjohn (2008) advanced a statistical classification algorithm in which the time-series responses were fitted with the Autoregressive Moving Average (ARMA) models and the ARMA coefficients were fed to the classifier, which was proved to be capable of learning in an unsupervised manner and of forming new classes when the structural response exhibits change. Lam and Ng (2006, 2008) put forward to a pattern recognition approach for the structural damage detection that used damage-induced changes in the Ritz vectors as the features to characterize the damage patterns defined by the corresponding locations and severity of damage. Unlike most other pattern recognition methods, the Bayesian ANN technique was employed as a tool for systematically identifying the damage pattern corresponding to an observed feature. The results of the case study demonstrated effectiveness of the proposed methodology. Chen and Zang (2009) developed an artificial immune pattern recognition (AIPR) approach for the damage classification, which incorporated several characteristics (adaptation, evolution, and immune learning) of the natural immune system and had been verified to classify structure damage patterns successfully by using a benchmark structure proposed by the American society of civil engineers (ASCE) structural health monitoring (SHM) task group and a three-story frame provided by the Los Alamos national laboratory. Zheng and Mita (2009) used the ARMA models in a two-stage damage assessment method where differences between the ARMA models were calculated as their Itakura distances, model cepstra or subspace angle distances used as damage detection features, and enhanced localization performance was achieved using pre-whitening filters. The approaches were applied to numerically simulated and experimental laboratory data. Lautour and Omenzetter (2010) developed a method for damage classification and estimation of remaining stiffness using the AR models and ANNs which had been applied to a simple 3-storey bookshelf structure and more complex ASCE Phase II

experimental SHM benchmark structure. The results showed that the combination of AR models and ANNs were efficient tools for damage classification and estimation, and performed well using small number of damage-sensitive features and limited sensors. Based on sequential application of an extended Kalman estimator for recursive solution of extended state vector and least-square estimation of unknown excitation inputs, Lei *et al.* (2012) proposed an algorithm for detecting structural damage with limited excitation input and response output measurement signals. Numerical study results showed that the proposed algorithm could identify structural parameters and unknown excitation in a sequential manner, which simplified the identification problem compared to other approaches available.

Although aforementioned methods have demonstrated various degrees of success in damage diagnosis of certain structures, engineers are still far from obtaining a framework that effectively detects damage in structures that were excited by a natural phenomenon, or have suffered from regular daily use and display conditions such as corrosion or fatigue, all within a reasonable budget. In this paper, a multi-stage approach for the damage diagnosis is investigated by use of the combined wavelet packet analysis and ANN. In the process of analysis, the time domain response signals are transformed by the WPT to obtain the damage-sensitive features. And then, by using the component energy in different frequency bands as the sample of the ANN can perfectly reflect the damage features. Following that, the ASCE benchmark structure is applied as numerical example for describing the process of the damage diagnosis. Finally, a few concluding remarks are given.

2. Multi-stage structural damage diagnosis method

It is desirable that different degrees and types of damage be identified accurately as they occur regardless of influencing factors that may affect the structural behavior. However, it is unrealistic that a single technique would be capable of detecting the damage of different degrees and types.

Therefore, a combination of methodologies that could optimally combines their outputs and takes full advantage of the information available should be the final goal of research in this area.

2.1. Wavelet packet analysis based energy extraction method

As known, the damage generally produces changes in the stiffness of a structure. These changes are reflected by changes in some of the dynamic properties. Thus, the focus of damage diagnosis is on feature extraction for a structure when subjected to dynamic excitation. The conventional feature extraction approach has generally relied upon the Fourier-based analysis as a means of translating vibration signals in the time domain into the frequency domain. However, the Fourier analysis provides a poor representation of signals well localized in time. Here, the WPT is introduced as an alternative means of extracting time-frequency information from the vibration signature. The WPT is an expansion of the discrete wavelet transform (DWT) that presents more possibilities for the signal processing (Misiti *et al.* 2004). Instead of just decomposing the low frequency component, it is possible to subdivide the whole time-frequency plane into different time-frequency pieces as can be seen from Fig. 1. The top level of the WPT is the time representation of signal, whereas, the bottom level has better frequency resolution. Thus, with the use of WPT, a better time-frequency resolution can be obtained for the decomposed signal.

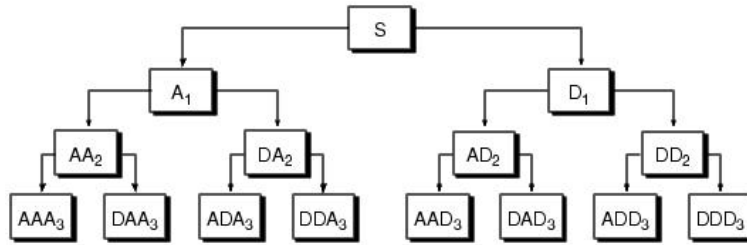


Fig.1 Three-tier factorization trees of wavelet packet transform

From the aforementioned discussion, it can be concluded that wavelet packets are a collection of function $\{2^{j/2}\Psi^i(2^j t - k)\}$, $i, j, k \in N$, generated from the following sequence of functions (Sun and Chang 2002, Wickerhauser 1994)

$$\Psi^{2i}(t) = \sqrt{2} \sum_k h(k) \Psi^i(2t - k) \tag{1}$$

$$\Psi^{2i+1}(t) = \sqrt{2} \sum_k g(k) \Psi^i(2t - k) \tag{2}$$

where $h(k)$ and $g(k)$ are the scaling and mother wavelet functions, respectively.

After the j th level of decomposition, the original signal $f(t)$ can be expressed as:

$$f(t) = \sum_{i=1}^{2^j} f_j^i(t) \tag{3}$$

The wavelet packet component signal $f_j^i(t)$ can be expressed by a linear combination of wavelet packet functions $\Psi_{j,k}^i(t)$ as follows

$$f_j^i(t) = \sum_k c_{j,k}^i \Psi_{j,k}^i(t) \tag{4}$$

The wavelet packet coefficient $c_{j,k}^i$ can be obtained from

$$c_{j,k}^i = \int_{-\infty}^{\infty} f(t) \Psi_{j,k}^i(t) dt \tag{5}$$

Providing that the wavelet packet functions are orthogonal

$$\Psi_{j,k}^m(t) \Psi_{j,k}^n(t) = 0 \text{ if } m \neq n \tag{6}$$

Each component in the WPT tree can be viewed as the output of a filter tuned to a particular basis function, thus the whole tree can be regarded as a filter bank. Since the breakage differently reacts on the every frequency component of the original signal, the frequency components will redistribute on the signal. The WPT actually decomposes the signal to different levels, which represent different frequency bands. This is to say, the feature vectors can be formed by extracting the energy of each level as the index of damage case. Yen and Lin (2000) define the wavelet packet component energy and concluded that it could provide a more robust signal feature for

classification than using the wavelet packet coefficients directly. The signal energy can be defined as follows

$$E_f = \int_{-\infty}^{\infty} f^2(t)dt = \sum_{m=1}^{2j} \sum_{n=1}^{2j} \int_{-\infty}^{\infty} f_j^m(t)f_j^n(t)dt \tag{7}$$

Substituting Eq. (4) into Eq. (7) and using the orthogonal condition, Eq. (6), gives

$$E_f = \sum_{i=1}^{2j} E_{f_j^i} \tag{8}$$

Where the wavelet packet component energy $E_{f_j^i}$ can be considered to be the energy stored in the component signal f_j^i

$$E_{f_j^i} = \int_{-\infty}^{\infty} f_j^i(t)^2 dt \tag{9}$$

It can be seen from Eq. (8) that the total signal energy can be decomposed into a summation of wavelet packet component energies that correspond to different frequency bands. Thus, if the response of structure under the external excitation is taken as the system output signal, the change of its energy of each frequency band can denote the damage state of some component of the structure (Sun and Chang 2002). The “energy-damage” principle presented here is just based on this point.

2.2. Improved BP neural network based damage detection algorithm

The ANN is a multiple network which is arranged logically by fundamental units that simulate the neuron activity in living brains. The information passing between the units simulates the function of a human brain nerve network; such as learning, recalling, concluding and speculating. Contrary to the traditional model-based methods, the ANN is a data-driven and self-adaptive method in which there are a few priori assumptions about the models for problems in the study. They learn from examples and capture subtle functional relations among the data even if the underlying relations are unknown or difficult to be described (Zhang *et al.* 2009).

A variety of different neural network models have been developed, among which the back-propagation (BP) network is the most widely adopted one. A typical BP neural network model is a full-connected neural network including input layer, hidden layer and output layer (Yang *et al.* 2009). The training of the learning process starts when a signal is transmitted from the hidden layer to the output layer. The training of a learning process has two phases, a forward propagation and backward propagation. Forward propagation is the first phase, which is a positive step from the first layer to the last. The weighted value and threshold value of each layer is calculated by iteration and passed into the BP three-layer network. The backward propagation is the second phase, where the weighted value and threshold values are revised. It is based on the impact of total error which is developed by calculating each weight and threshold value from the final layer backwards to the first one. These two phases operate repeatedly and alternately until they converge. After this training process, the network can “distinguish” and “remember” the raw data. When the network is stimulated by actions similar to those previously learnt its output section can give corresponding results. Thus, the ANN is well suited for damage identification problems whose solutions require knowledge that be difficult to specify and in which there are

enough data or observations.

However, the basic BP algorithm is too slow for practical applications of the damage identification. In order to speed up the algorithm and make it more practical, several modifications have been proposed by researchers (Basheer and Hajmeer 2000, Song 2000). The research on faster algorithm falls roughly into two categories. One involves the development of heuristic techniques such as the use of momentum and variable learning rates. The other has focused on standard numerical optimization techniques such as the conjugate gradient algorithm and the Levenberg-Marquardt algorithm. Among these algorithms, the Levenberg-Marquardt algorithm is most rapid for medium networks. So, this paper adopts the BP network in combination with the Levenberg-Marquardt algorithm.

2.3. Outline of multi-stage structural damage diagnosis method

Generally, the ANN can identify the type, location and grade at the same time. However, if the structure is complex, the sample amount for training would be excessively large and the training time has further to be exceedingly long. Thus, a multi-stage damage detection method is adopted here, and the occurrence, location and severe grade of the damage are diagnosed, respectively. The multi-stage method based on the WPT and the improved BP network is given as follows:

Step (1): Decompose the signal of the structural response to be detected to the rational level through a trial and error sensitivity analysis using the healthy and damaged structural models.

Step (2): Extract the signal of the different bands and calculate the wavelet packet component energies in each frequency band.

Step (3): Select the wavelet packet component energy which is significant in actual value and damage sensitive to construct the feature vector.

Step (4): Put the feature vectors constructed into the ANN to diagnose the whether the structure is damaged.

Step (5): Put the feature vectors selected into the ANN to locate the structure damage.

Step (6): Put the feature vectors selected into the ANN to quantity the structure damage.

3. Damage diagnosis for the ASCE benchmark structure

In order to test and compare various damage identification techniques, a benchmark problem was proposed by the ASCE task group on health monitoring (Johnson *et al.* 2004). The benchmark structure is a four-story, two-bay by two-bay steel-frame scale model structure built in the earthquake engineering research laboratory at the University of British Columbia, Canada. It has a 2.5 m×2.5 m plan and is 3.6 m tall. Each story is composed of 9 columns of 0.9 m each in height, 12 beams of 1.25 m each in length, 8 lateral braces, and 4 floor weights. A diagram for the analytical model for the benchmark structure is shown in Fig. 2(a), giving dimensions and coordinate directions in which the x direction is the strong direction of the columns.

Fig. 2(b) illustrates node numbering in the finite element (FE) model of the benchmark structure. The columns and floor beams are modeled as the Euler-Bernoulli beams in the FE model.

The braces are bars with no bending stiffness. The FE model, by removing the stiffness of various elements, can simulate damage to the structure. The excitations are applied to each floor, which are modeled as the filtered Gaussian white noise processes passing through the 6th-order

low-pass Butterworth filter with a 100 Hz cutoff, and the sampling frequency is 1000 Hz. The response of the structure in y direction at top center (node 41) is selected to analysis.

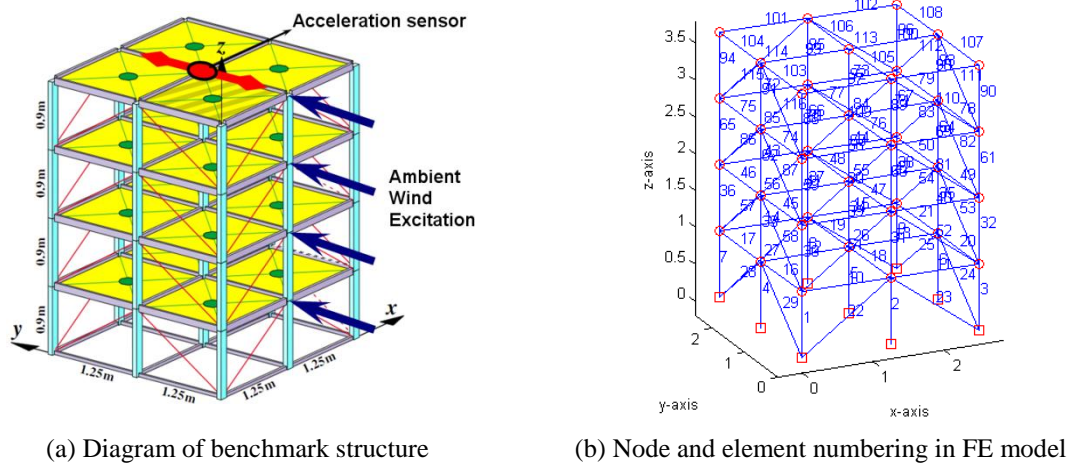


Fig. 2 ASCE SHM benchmark structure

Table 1 Ten damage patterns considered in the benchmark structure study

Damage pattern	Description
1	All braces are removed in each story
2	Two braces at the same side are removed in each story
3	2/3 loss of stiffness on two braces at the same side in each story
4	1/3 loss of stiffness on two braces at the same side in each story
5	Two braces at the different sides are removed in each story
6	2/3 loss of stiffness on two braces at the different sides in each story
7	1/3 loss of stiffness on two braces at the different sides in each story
8	One brace are removed in each story
9	2/3 loss of stiffness on one brace at the different sides in each story
10	1/3 loss of stiffness on one brace at the different sides in each story

3.1. Determining damage of structure

For the excitation of the ambient wind loading in the y direction, the damage of brace in the x direction has so little affection on the dynamic response of stories in which only the damage cases of the brace in the y direction are considered here. As shown in Table 1, a total of 10 damage scenarios are simulated on the structure, which give a mixture of extensive damage patterns by involving the loss of stiffness on braces or the removal bracing in various combinations.

There are many wavelet functions that could form the WP, such as “db”, “haar”, “sym” and “coif”. The choice of the WP function for the aforementioned procedure is theoretically arbitrary, but it is critical and important in practice, because it affects the performance of the technique. In this paper, the Daubechies 6 (db6) WP in the MATLAB Wavelet Toolbox (MathWorks, Natick,

MA, USA) was found to perform better by the trial and error. In addition, a sufficiently high level of decomposition should be used in order to have sensitive component energies. For this example, the decomposition level is set to 6 through the sensitivity analysis, which generate a total of 64 component energies. As shown in Fig. 3, the first 12 component energies identified by asterisks are selected according to their magnitudes to form the feature vector for the neural network.

The outputs of ANN model have the corresponding information with the damage as follows: undamaged pattern (1 0 0 0 0), the damage occurrence on the 1st story (0 1 0 0 0), the damage occurrence on the 2nd story (0 0 1 0 0), the damage occurrence on the 3rd story (0 0 0 1 0), and the damage occurrence on the 4th story (0 0 0 0 1). Some researchers claim that the network with a single hidden layer can approximate any continuous function to any desired accuracy and is enough for most forecasting problems (Li and Sun 2003). Thus, a three-layer neural network (called ANN model-1) is applied in the damage detection, which can be designed as a 12-nodes input layer, a 9-nodes hidden layer and a 5-nodes output layer. The aforementioned Levenberg-Marquardt algorithm is adopted to train the network. In computation, its precision had reached 10^{-7} when the number of iteration was 64. The 10 patterns produce 60 sample groups, and then there are 61 groups together with the undamaged pattern, among them some for training and some for testing. The part of the trained results is shown as Table 2. The 8 testing groups are input into the ANN model-1 after being trained, and the diagnostic results are illustrated in Table 3. As shown in Table 3, the identified precision of the ANN model-1 is very well. The diagnostic results of the unknown patterns are correct and the trained periods are short enough to be accepted for the on-line monitoring.

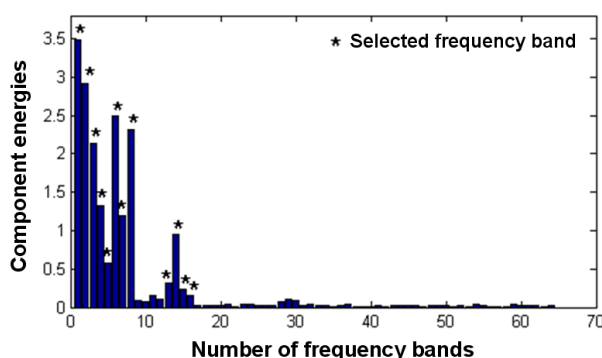


Fig. 3 WP component energies and its selection result of the ANN model-1

Table 2 Some trained results of ANN model-1

Sample number	Damage story	Target vector	Trained result					Error (%)
1	0	1 0 0 0 0	1.0000	-0.0001	0.0000	0.0001	0.0000	0.00
2	1	0 1 0 0 0	0.0003	1.0000	-0.0001	-0.0000	-0.0002	0.02
3	2	0 0 1 0 0	0.0001	-0.0001	0.9995	0.0003	0.0001	0.03
4	3	0 0 0 1 0	-0.0000	-0.0000	-0.0000	1.0000	0.0000	0.00
5	4	0 0 0 0 1	0.0000	-0.0002	0.0002	0.0002	0.9998	0.02
6	1	0 1 0 0 0	0.0003	1.0000	-0.0001	-0.0001	-0.0001	0.02
7	2	0 0 1 0 0	0.0000	0.0004	1.0000	-0.0005	-0.0000	0.03
8	3	0 0 0 1 0	-0.0000	-0.0001	-0.0001	1.0002	0.0000	0.01
9	4	0 0 0 0 1	0.0000	-0.0001	0.0000	0.0000	0.9999	0.00

Table 3 Diagnostic results of ANN model-1

Sample number	Diagnostic target	Diagnostic result					Damage story	Error (%)	Conclusion
1	0 1 0 0 0	0.0004	0.9989	0.0005	0.0007	-0.0006	1	0.07	correct
2	0 0 0 1 0	-0.0000	-0.0000	-0.0001	1.0002	-0.0001	3	0.01	correct
3	0 0 0 1 0	0.0001	-0.0002	0.0006	0.9989	0.0006	3	0.06	correct
4	0 0 0 0 1	0.0000	-0.0003	0.0002	0.0002	0.9998	4	0.02	correct
5	0 0 0 1 0	-0.0000	-0.0001	-0.0000	1.0001	-0.0000	3	0.00	correct
6	0 0 0 0 1	-0.0000	0.0001	-0.0001	-0.0001	1.0001	4	0.01	correct
7	0 1 0 0 0	-0.0008	1.0013	-0.0002	-0.0000	-0.0002	1	0.07	correct
8	0 0 1 0 0	-0.0000	0.0001	0.9997	-0.0004	0.0002	2	0.03	correct

3.2. Quantifying the severity of damage

From section 3.1, one can judge that on which story the damage occurs. Then the damage information of that story is further used as the new patterns for the ANN model-2 training. To quantify the severity of damage, 6 degrees of the damage are partitioned as Table 4 according to the damage patterns aforementioned.

Table 4 Six damage degrees partitioned according to the damage pattern

Code of damage degree	Corresponding damage pattern	Code of ANN model-1 output layer	Damage degree
d1	Pattern (1)	1 0 0 0 0 0	extremely severe
d2	Pattern (2), (5)	0 1 0 0 0 0	severe
d3	Pattern (3), (6)	0 0 1 0 0 0	moderate
d4	Pattern (8)	0 0 0 1 0 0	generic
d5	Pattern (4), (7), (9)	0 0 0 0 1 0	minor
d6	Pattern (10)	0 0 0 0 0 1	slight

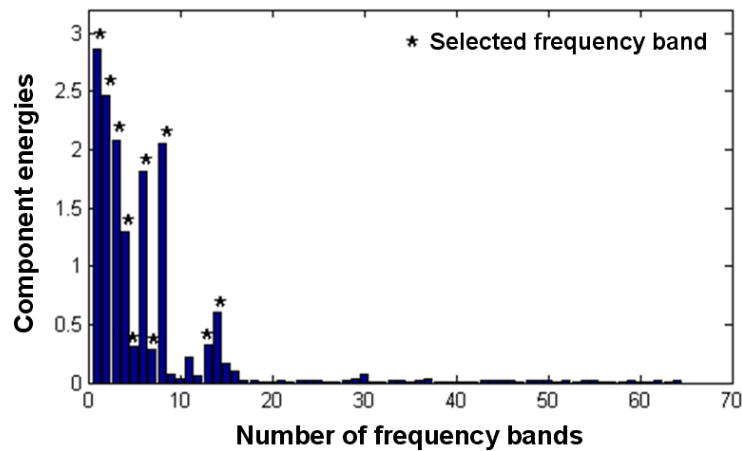


Fig. 4 WP component energies and its selection result of the ANN model-2

To take the 3rd story of the benchmark structure for an example, there are totally 16 damaged patterns that are divided into two parts: 14 patterns for training and 2 patterns for testing. For the new ANN model (called ANN model-2), it is composed of a 10-nodes input layer, a 15-nodes hidden layer and a 6-nodes output layer, which is still trained by the Levenberg-Marquardt algorithm. Accordingly, the first 10 component energies identified by asterisks in Fig. 4 are selected on the base of their magnitude to form the feature vector for the neural network. The trained results are demonstrated as Table 5. Two testing patterns are then input into the ANN model-2 after being trained, and the diagnostic results are listed in Table 6. It can be found from Table 6 that the well-trained ANN model-2 can make the correct diagnosis extended to the other unknown patterns.

Table 5 Trained results of ANN model-2

Sample number	Code of damage degree	Target vector	Trained result							Error (%)
1	d1	1 0 0 0 0 0	1.0000	0.0000	0.0000	-0.0000	-0.0000	-0.0000	0.00	
2	d2	0 1 0 0 0 0	0.0001	1.0002	0.0002	-0.0003	-0.0001	0.0001	0.02	
3	d2	0 1 0 0 0 0	-0.0001	0.9998	-0.0002	0.0003	0.0001	-0.0001	0.02	
4	d5	0 0 0 0 1 0	-0.0001	0.0000	-0.0002	-0.0002	1.0000	0.0003	0.02	
5	d5	0 0 0 0 1 0	-0.0001	0.0000	-0.0002	-0.0001	0.9998	0.0004	0.02	
6	d3	0 0 1 0 0 0	0.0001	-0.0005	0.9997	0.0003	-0.0003	0.0008	0.05	
7	d3	0 0 1 0 0 0	-0.0000	-0.0000	0.9999	-0.0000	0.0000	0.0001	0.01	
8	d5	0 0 0 0 1 0	-0.0001	0.0000	-0.0002	-0.0001	0.9998	0.0004	0.02	
9	d3	0 0 1 0 0 0	-0.0001	0.0005	1.0004	-0.0003	0.0003	-0.0009	0.05	
10	d4	0 0 0 1 0 0	0.0001	-0.0001	-0.0000	0.9999	0.0001	-0.0000	0.02	
11	d4	0 0 0 1 0 0	-0.0001	0.0001	0.0000	1.0001	-0.0001	0.0000	0.01	
12	d6	0 0 0 0 0 1	-0.0000	-0.0000	0.0000	-0.0000	0.0010	0.9991	0.06	
13	d6	0 0 0 0 0 1	-0.0000	0.0000	-0.0000	0.0000	-0.0006	1.0006	0.04	
14	d5	0 0 0 0 1 0	0.0002	-0.0001	0.0005	0.0004	1.0003	-0.0011	0.06	

Table 6 Diagnostic results of ANN model-2

Sample number	Diagnostic target	Diagnostic result							Code of damage degree	Error (%)	Conclusion
1	0 0 1 0 0 0	0.0002	-0.0005	0.9998	0.0004	-0.0004	0.0007	d3	0.05	Correct	
2	0 0 0 0 1 0	0.0003	-0.0001	0.0005	0.0005	1.0003	-0.0011	d5	0.06	Correct	

3.3. Locating the damage

According to the diagnosis process described in section 3.1 and 3.2, one can judge that on which story the damage occurs and what the damage severity is. However, the aforementioned process cannot determine the specific damage location. For instance, in Fig. 5 the damage in the first story may occur at the negative or positive direction of x axis or at both two sides. To estimate that at which side the damage occurs, the accelerations are selected in the y direction of

nodes 13 and 15 as the signals to be analyzed. There are 16 damage patterns, in which the 2 patterns are chosen for testing and the remains are input into the ANN model-3 for training. The designed ANN model-3 consists of a 16-node input layer, a 15-node hidden layer and a 2-node output layer, which is trained by the Levenberg-Marquardt algorithm too. The WP component energies and its selection result of the ANN model-3 is demonstrated in Fig. 6. The trained results are listed in Table 7. And two testing patterns are put into the ANN model-3 after being trained; the detection results are shown in Table 8. The results in the Tables 7 and 8 indicate that the errors of diagnosis results are relatively big compared to the trained results. Yet, such errors can indeed satisfy the need for the practical engineering.

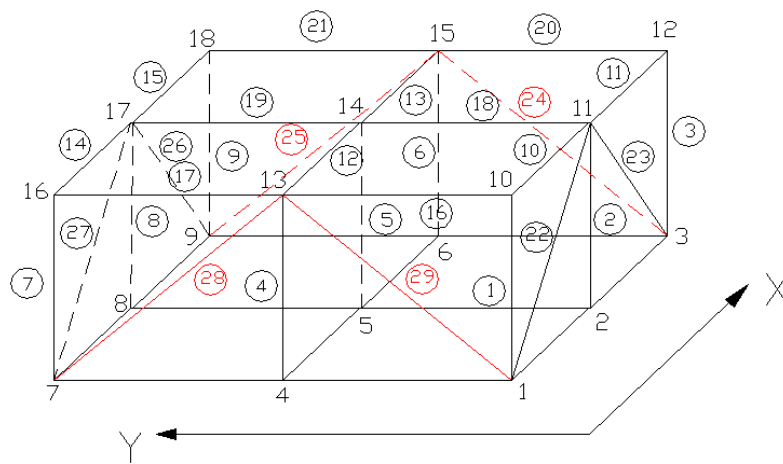


Fig. 5 Damaged braces in the first story of the structure

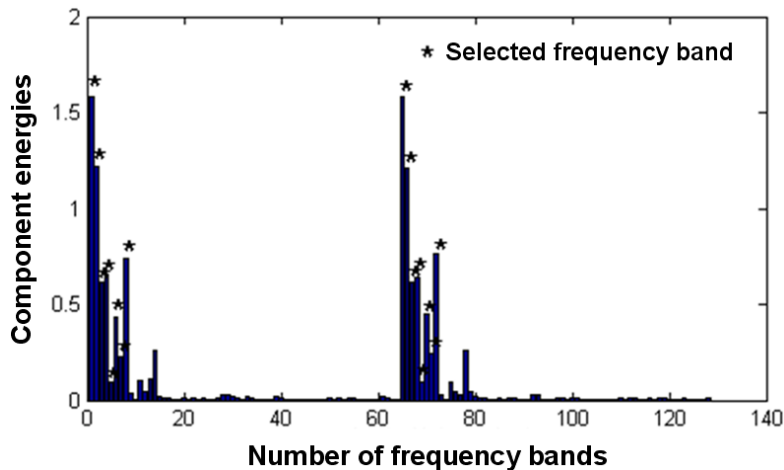


Fig. 6 WP component energies and its selection result of the ANN model-3

Table 7 Trained results of ANN model-3

Sample number	Target vector	Damage location in x axis	Trained result	Error (%)
1	1 0	“-”	1.0000 0.0000	0.00
2	0 1	“+”	0.0000 1.0000	0.00
3	1 0	“-”	1.0000 0.0000	0.00
4	0 1	“+”	-0.0000 1.0000	0.00
5	1 1	“+”, “-”	1.0000 1.0000	0.00
6	0 1	“+”	0.0000 1.0000	0.00
7	1 0	“-”	1.0000 -0.0000	0.00
8	0 1	“+”	-0.0002 1.0000	0.01
9	1 0	“-”	1.0000 -0.0000	0.00
10	0 1	“+”	0.0000 1.0000	0.00
11	1 0	“-”	1.0000 -0.0000	0.00
12	1 1	“+”, “-”	0.9987 1.0000	0.09
13	1 1	“+”, “-”	1.0000 1.0000	0.00

Table 8 Diagnostic results of ANN model-3

Sample number	Diagnostic target	Diagnostic result	Damage location in x axis	Error (%)	Conclusion
1	1 0	0.9989 -0.0000	“-”	0.08	Correct
2	0 1	0.0239 1.0000	“+”	1.69	Correct

3.4. Network generalization ability test

After the ANNs are trained successfully, all domain knowledge extracted out from the existing samples is stored as digital forms in weights associated with each connection between neurons. Although the verified results in Tables 3, 6 and 8 show that the well-trained network models take on optimal generalization performance, these validation data sets have the same damage patterns to training data sets. Thus, it is worth paying attention to evaluate whether there is a big difference between the output and target value when using totally different testing set obtained from other damage patterns, which represent the generalization capability of these BP models for decision making. Here, 1/5, 2/5, 3/5 and 4/5 loss of stiffness on the lateral brace were simulated to generate 20 new testing sets.

The generalization ability test results of ANN model-1 are shown in Table 9. It can be easily found that except sample numbers 1, 5, 9 and 17, the differences between the diagnostic and target value are less than 0.5% that means the ANN model-1 has good generalization capability.

The results in Table 10 indicate that there are differences between the targets and the diagnosis results for the ANN model-2. These are caused by the fact that only 6 degrees of the damage are partitioned, i.e., the damage pattern divided too rough. However, for an actual project, it is impossible to finely divide all of the damage levels. Thus, the generalization performance of the trained network can be thought to be good if the damage level could be diagnosed in relatively accurate. The results in Tab.11 indicate that except sample 2 the errors of the diagnosis results are relatively small compared to the targets.

Table 9 Generalization ability test results of ANN model-1

Sample number	Diagnostic target	Diagnostic result					Damage story	Error (%)	Conclusion
1	0 1 0 0 0	0.0678	0.9241	0.0003	0.0064	0.0013	1	4.56	Correct
2	0 1 0 0 0	0.0002	0.9995	0.0006	-0.000	-0.0001	1	0.04	Correct
3	0 1 0 0 0	-0.0030	1.0039	0.0002	-0.0010	-0.0001	1	0.22	Correct
4	0 1 0 0 0	0.0002	1.0001	-0.0001	0.0001	-0.0002	1	0.01	Correct
5	0 0 1 0 0	0.0392	0.1050	0.8506	0.0021	0.0030	2	8.35	Correct
6	0 0 1 0 0	-0.0000	-0.0003	1.0001	-0.0001	0.0002	2	0.02	Correct
7	0 0 1 0 0	-0.0004	0.0008	0.9997	0.0002	-0.0002	2	0.04	Correct
8	0 0 1 0 0	-0.0000	0.0001	1.0002	-0.0001	-0.0002	2	0.01	Correct
9	0 0 0 1 0	0.1468	-0.0410	-0.0017	0.9120	-0.0161	3	7.90	Correct
10	0 0 0 1 0	-0.0020	-0.0016	0.0006	1.0012	0.0017	3	0.15	Correct
11	0 0 0 1 0	-0.0004	-0.0005	0.0001	1.0005	0.0004	3	0.04	Correct
12	0 0 0 1 0	-0.0000	0.0003	-0.0001	1.0001	-0.0003	3	0.02	Correct
13	0 0 0 1 0	-0.0020	-0.0014	0.0006	1.0012	0.0016	3	0.14	Correct
14	0 0 0 1 0	-0.0001	0.0003	-0.0001	1.0002	-0.0003	3	0.02	Correct
15	0 0 0 1 0	0.0001	0.0001	-0.0001	0.9999	-0.0001	3	0.01	Correct
16	0 0 0 1 0	0.0002	0.0001	-0.0001	0.9999	-0.0001	3	0.01	Correct
17	0 0 0 0 1	0.0689	0.2577	-0.0000	0.0052	0.6683	4	19.04	Correct
18	0 0 0 0 1	0.0000	0.0000	-0.0001	0.0000	1.0000	4	0.00	Correct
19	0 0 0 0 1	-0.0005	-0.0017	0.0002	-0.0001	1.0021	4	0.12	Correct
20	0 0 0 0 1	0.0000	0.0001	-0.0001	0.0000	0.9999	4	0.01	Correct

Table 10 Generalization ability test results of ANN model-2

Sample number	Diagnostic target	Diagnostic result						Damage degree	Error (%)	Conclusion
82-1/5	0 0 0 0 1	-0.0015	0.0006	-0.0016	-0.0005	-0.1167	1.1187	d6	6.80	Correct
82-2/5	0 0 0 0 1 0	-0.0001	0.0001	-0.0005	0.0000	0.3426	0.6578	d6	19.8	Correct
82-3/5	0 0 0 0 1 0	-0.0004	0.0002	-0.0009	-0.0002	0.9957	0.0052	d5	0.28	Correct
82-4/5	0 0 0 0 1 0	0.0299	-0.0179	-0.0613	0.1897	0.9025	-0.0112	d5	9.18	Correct
8283-1/5	0 0 0 0 1	-0.0001	0.0000	-0.0004	0.0000	0.2726	0.7276	d6	15.73	Correct
8283-2/5	0 0 0 0 1 0	0.0091	-0.0054	-0.0102	0.0487	0.9724	-0.0049	d5	2.37	Correct
8283-3/5	0 0 1 0 0 0	-0.0343	0.0204	0.8489	0.1007	0.0170	0.0109	d3	7.63	Correct
8283-4/5	0 0 1 0 0 0	0.0073	-0.0059	1.0212	-0.0102	-0.0045	-0.0000	d3	1.05	Correct

Table 11 Generalization ability test results of ANN model-3

Sample number	Diagnostic target		Diagnostic result		Damage location in x axis	Error (%)	Conclusion
1	1	0	1.0000	0.0000	“-”	0.00	Correct
2	1	0	1.0000	0.1876	“-”	13.27	Correct
3	0	1	-0.0000	1.0000	“+”	0.00	Correct
4	0	1	0.0129	1.0001	“+”	0.91	Correct
5	1	0	1.0000	0.0000	“-”	0.00	Correct
6	1	0	1.0000	0.0009	“-”	0.06	Correct
7	0	1	-0.0000	1.0000	“+”	0.00	Correct
8	0	1	-0.0000	1.0000	“+”	0.00	Correct

Table 12 Anti-noise performance test results

Damage sample	Diagnostic target	Noise level	Diagnostic result					Error (%)
Brace 28 and 29 in first story are removed	0 1 0 0 0	10%	0.0004	0.9989	0.0005	0.0007	-0.0006	0.07
		15%	0.0001	1.0018	-0.0012	0.0002	-0.0009	0.10
		20%	-0.0001	1.0074	-0.0020	0.0011	-0.0064	0.45
Brace 86 in third story is removed	0 0 0 1 0	10%	-0.0000	-0.0000	-0.0001	1.0002	-0.0001	0.01
		15%	0.0001	-0.0018	-0.0001	0.9999	0.0019	0.12
		20%	0.0001	-0.0110	-0.0001	0.9999	0.0111	0.70
1/3 loss of stiffness on brace 116 at the fourth story	0 0 0 0 1	10%	0.0000	-0.0003	0.0002	0.0002	0.9998	0.02
		15%	0.0008	-0.0045	0.0004	-0.0014	1.0016	0.22
		20%	0.0010	0.0039	-0.0007	-0.0008	0.9966	0.24
2/3 loss of stiffness on brace 87 at the third story	0 0 0 1 0	10%	-0.0000	-0.0001	-0.0000	1.0001	-0.0000	0.00
		15%	-0.0002	-0.0018	-0.0001	1.0002	0.0018	0.11
		20%	-0.0012	-0.0075	-0.0003	1.0005	0.0086	0.51
2/3 loss of stiffness on brace 116 at the fourth story	0 0 0 0 1	10%	-0.0000	0.0001	-0.0001	-0.0001	1.0001	0.01
		15%	0.0001	-0.0001	0.0000	-0.0001	1.0001	0.01
		20%	0.0001	-0.0001	-0.0001	0.0000	1.0001	0.01
1/3 loss of stiffness on brace 28 and 29 at the first story	0 1 0 0 0	10%	-0.0008	1.0013	-0.0002	-0.0000	-0.0002	0.07
		15%	0.0014	1.0047	-0.0040	0.0002	-0.0023	0.30
		20%	0.0004	1.0178	-0.0098	0.0060	-0.0145	1.15
2/3 loss of stiffness on brace 57 and 58 at the second story	0 0 1 0 0	10%	-0.0000	0.0001	0.9997	-0.0004	0.0005	0.03
		15%	-0.0000	-0.0007	1.0002	-0.0001	0.0006	0.04
		20%	0.0000	-0.0035	1.0001	-0.0001	0.0035	0.22

3.5. Network anti-noise performance test

As known, the noise embedded in measured signals, sometimes even very heavy, disturbs the reliability and accuracy of measurements, and thus places a fundamental limit on the detection of small damages. Therefore, the anti-noise performance of the network should be tested carefully.

The measurement noise is introduced in the structural responses to discuss the effect of the noise on the damage diagnosis. The noise level is determined by the percentage of the maximum root-mean-square of top responses. Here, the data of 10% noise is used for network training, and three groups of test samples (each has 7 samples) with 10%, 15% and 20% noises are used for testing the network anti-noise performance. The comparisons of the diagnostic errors are shown in Table 12 and the comparison curves are shown in Fig. 7. From Table 12 and Fig. 7, it can be seen

that with the increase of noise levels, the network diagnostic errors increase. However, even at the 20% noise level, the error is no more than 2%, which fully satisfies the engineering requirement. Thereby, the method can produce correct results under conditions of heavy noise, which is an effective method for damage diagnosis.

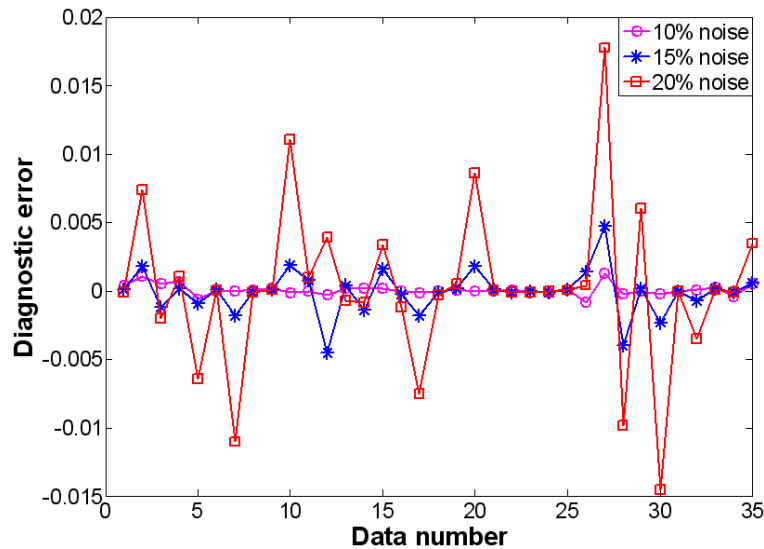


Fig. 7 Diagnostic error of the network under different noise levels

4. Conclusions

Despite vibration-based structural damage detection methods have attracted considerable attention over the past decade, robust and reliable methods capable of detecting, locating and estimating damage whilst being insensitive to changes in environmental and operating conditions have yet to be agreed upon. This paper investigated the multi-stage structural damage diagnosis method for the steel frame structure. Based on the numerical results, the following observations can be obtained:

(1) It is unrealistic that a single technique would be capable of detecting damage of different degrees and types. The WPT-based feature extraction procedure could obtain useful information for the damage assessment and ANN is well suited for the damage identification with the reasonable accuracy which does not seem to be affected by presence of measurement noise. The combined use of the WPT and ANN model is promising for the damage diagnosis of structures.

(2) The multi-stage structural damage diagnosis method has been used to classify minor, moderate and severe structure damage patterns using a benchmark structure proposed by the ASCE SHM Task Group. The results are very encouraging. Regardless of minor, moderate or severe stiffness reductions, most of the damages identified by trained ANNs are very close to the true values.

(3) The preliminary damage detection procedure summarized in this paper is not

time-consuming which may be on-line applied in the in-situ condition if the off-line analysis of the component energy and training of the ANN model have been finished.

Acknowledgements

This research work was jointly supported by the Science Fund for Creative Research Groups of the NSFC (Grant No. 51121005), the “973” Project (Grant No. 2011CB013605), the National Natural Science Foundation of China (Grant No. 91315301, 51222806, 51310105008), the Fundamental Research Funds for Central Universities (Grant No. DUT13YQ105), and the Research Fund of State Key Laboratory of Coastal and Offshore Engineering (Grant No. SL2012-6).

References

- Basheer, I.A. and Hajmeer, M. (2000), “Artificial neural networks: Fundamentals, computing, design, and application”, *J. Microbiol. Meth.*, **43**(1), 3-31.
- Boller, C., Chang, F.K. and Fujino, Y. (2009), *Encyclopedia of structural health monitoring*, John Wiley & Sons Ltd.
- Carden, E.P. and Brownjohn, J.M.W. (2008), “ARMA modelled time-series classification for structural health monitoring of civil infrastructure”, *Mech. Syst. Signal Pr.*, **22**(2), 295-314.
- Chen, B. and Zang, C.Z. (2009), “Artificial immune pattern recognition for structure damage classification”, *Comput. Struct.*, **87**(21-22), 1394-1407.
- Doebling, S.W., Farrar, C.R., Prime, M.B. and Shevitz, D.W. (1996), *Damage identification and health monitoring of structural and mechanical systems from changes in their vibration characteristics: a literature review*, Los Alamos National Laboratory Report, LA-13070-MS.
- Johnson, E.A., Lam, H.F., Katafygiotis, L.S. and Beck, J.L. (2004), “Phase I IASC-ASCE structural health monitoring benchmark problem using simulated data”, *J. Eng. Mech. - ASCE*, **130**(1), 3-15.
- Lam, H.F. and Ng, C.T. (2008), “The selection of pattern features for structural damage detection using an extended Bayesian ANN algorithm”, *Eng. Struct.*, **30**(10), 2762-2770.
- Lam, H.F., Yuen, K.V. and Beck, J.L. (2006), “Structural health monitoring via measured Ritz vectors utilizing artificial neural networks”, *Comput. Aided Civ. Inf.*, **21**(4), 232-241.
- Lautour, O.R. and Omenzetter, P. (2010), “Damage classification and estimation in experimental structures using time series analysis and pattern recognition”, *Mech. Syst. Signal Pr.*, **24**(5), 1556-1569.
- Lei, Y., Jiang, Y.Q. and Xu, Z.Q. (2012), “Structural damage detection with limited input and output measurement signals”, *Mech. Syst. Signal Pr.*, **28**(0), 229-243.
- Li, H.N. and Sun, H.M. (2003), “Damage diagnosis of framework structure based on wavelet packet analysis and neural network”, *Earthq. Eng. Eng. Vib.*, **23**(5), 141-148.
- Li, H.N. and Yang H. (2007), “System identification of dynamic structure by the multi-branch BPNN”, *Neurocomputing*, **70**(4-6), 835-841.
- Misiti, M., Misiti, Y., Oppenheim, G. and Poggi, J.M. (2004), *Wavelet toolbox for use with Matlab, User's Guide*, Ver. 3.
- MATLAB, *The MathWorks*, Inc. Natick, MA (USA), <http://www.mathworks.com>.
- Nair, K.K., Kiremidjian, A.S. and Law, K.H. (2006), “Time series-based damage detection and localization algorithm with application to the ASCE benchmark structure”, *J. Sound Vib.*, **291**(1-2), 349-368.
- Sohn, H., Farrar, C.R., Hunter, N.F. and Worden, K. (2001), “Structural health monitoring using statistical pattern recognition techniques”, *J. Dyn. Syst. Meas. Control T.- ASME*, **23**(4), 706-711.
- Song, Y.B. (2000), “Quick training method for multi-layer bp neural network and its application”, *Contr.*

- Dec.*, **15**(1), 125-127.
- Sun, Z. and Chang, C.C. (2002), “Structural damage assessment based on wavelet packet transform”, *J. Struct. Eng. - ASCE*, **128**(10), 1354-1361.
- Wenzel, H. (2009), *Health monitoring of bridges*, USA, John Wiley and Sons Ltd.
- Wickerhauser M.V. (1994), *Adapted wavelet analysis-from theory to software*, (Ed. A.K. Peters), Wellesley, MA, USA.
- Yang, L.N., Peng, L., Zhang, L.M., Zhang, L.L. and Yang S.S. (2009), “A prediction model for population occurrence of paddy stem borer based on back propagation artificial neural network and principal components analysis”, *Comput. Electron. Agr.*, **68**(2), 200-206.
- Yen, G.G. and Lin, K.C. (2000), “Wavelet packet feature extraction for vibration monitoring”, *IEEE T. Ind. Electron.*, **47**(3), 650-667.
- Yi, T.H., Li, H.N. and Gu M. (2012), “Recent research and applications of GPS-based monitoring technology for high-rise structures”, *Struct. Health Monit.*, **20**(5), 649-670.
- Zhang, H., Schulz, M.J., Ferguson, F. and Pai, P.F. (1999), “Structural health monitoring using transmittance functions”, *Mech. Syst. Signal Pr.*, **13**(5), 765-787.
- Zhang, L., Luo, J.H. and Yang S.Y. (2009), “Forecasting box office revenue of movies with BP neural network”, *Expert Syst. Appl.*, **36**(3), 6580-6587.
- Zheng, H. and Mita, A. (2009), “Localized damage detection of structures subject to multiple ambient excitations using two distance measures for autoregressive models”, *Struct. Health Monit.*, **8**(3), 207-222.